

Published in final edited form as:

*Phys Med Biol.* 2015 February 7; 60(3): 1367–1383. doi:10.1088/0031-9155/60/3/1367.

## Measurement of gastric meal and secretion volumes using magnetic resonance imaging

C.L. Hoad<sup>1,2</sup>, H. Parker<sup>2</sup>, N. Hudders<sup>2</sup>, C. Costigan<sup>1</sup>, E.F. Cox<sup>1</sup>, A.C. Perkins<sup>3,4,5</sup>, P.E. Blackshaw<sup>4</sup>, L. Marciani<sup>2,5</sup>, R.C. Spiller<sup>2,4</sup>, M.R. Fox<sup>2,6</sup>, and P.A. Gowland<sup>1</sup>

<sup>1</sup>Sir Peter Mansfield Magnetic Resonance Centre, School of Physics and Astronomy, University of Nottingham

<sup>2</sup>NIHR Biomedical Research Unit in Gastrointestinal and Liver Diseases, Nottingham University Hospitals Trust and the University of Nottingham

<sup>3</sup>Medical Imaging Unit, School of Medicine, University of Nottingham, Nottingham UK

<sup>4</sup>Department of Medical Physics & Clinical Engineering, Nottingham University Hospitals, Nottingham, UK

<sup>5</sup>Nottingham Digestive Diseases Centre, School of Medicine, University of Nottingham, Nottingham, UK

### Abstract

MRI can assess multiple gastric functions without ionizing radiation. However, time consuming image acquisition and analysis of gastric volume data, plus confounding of gastric emptying measurements by gastric secretions mixed with the test meal have limited its use to research centres. This study presents an MRI acquisition protocol and analysis algorithm suitable for the clinical measurement of gastric volume and secretion volume. Reproducibility of gastric volume measurements was assessed using data from 10 healthy volunteers following a liquid test meal with rapid MRI acquisition within one breath-hold and semi-automated analysis. Dilution of the ingested meal with gastric secretion was estimated using a respiratory-triggered T<sub>1</sub> mapping protocol. Accuracy of the secretion volume measurements was assessed using data from 24 healthy volunteers following a mixed (liquid/solid) test meal with MRI meal volumes compared to data acquired using gamma scintigraphy (GS) on the same subjects studied on a separate study day. The mean (SD) coefficient of variance between 3 observers for both total gastric contents (including meal, secretions and air) and just the gastric contents (meal and secretion only) was 3 (2) % at large gastric volumes (> 200 ml). Mean (SD) secretion volumes post meal ingestion were 64 (51) ml and 110 (40) ml at 15 and 75 minutes respectively. Comparison with GS meal volumes, showed that MRI meal only volume (after correction for secretion volume) were similar to GS, with a linear regression gradient (std err) of 1.06 (0.10) and intercept -11 (24) ml. In conclusion, (i) rapid acquisition removed the requirement to image during prolonged breath-hold (ii) semi-automatic analysis greatly reduced time required to derive measurements and (iii) correction for secretion volumes provides accurate assessment of gastric meal volumes and emptying. Together

<sup>6</sup>iDigest: Zurich, Laboratory and Clinic for Disorders of Gastrointestinal Motility and Function, Division of Gastroenterology and Hepatology, University Hospital Zurich, Switzerland (current address)

these features provide the scientific basis of a protocol which would be suitable in clinical practice.

## Keywords

Gastric Volume; MRI; secretion

---

## Introduction

MRI is a very useful tool for studying both the structure and function of the stomach (Curcic et al., 2010, Marciani, 2011) as well as the mechanisms by which food is digested in and emptied from the stomach (Marciani et al., 2012, Marciani et al., 2013, Marciani et al., 2007, Kwiatek et al., 2009) A key advantage of MRI is that this techniques can acquire near simultaneous measurements of multiple parameters of gastric function in a single scanning session without ionizing radiation. Gastric emptying can be measured by the reduction in the volume of gastric contents over time on anatomical MRI scans (Fruehauf et al., 2009, Marciani et al., 2001b, Marciani et al., 2000, Schwizer et al., 1992, Steingoetter et al., 2006), gastric motility can be assessed using cine imaging (Borovicka et al., 1999, Kwiatek et al., 2006, Marciani et al., 2005, Marciani et al., 2001c) and gastric secretion can be estimated by monitoring the dilution of the meal (Sauter et al., 2012, Treier et al., 2008, Goetze et al., 2009). Based on these findings, gastric MRI has been proposed as a clinical investigation for the diagnosis of gastroesophageal reflux (Curcic et al., 2014a), gastroparesis (Ajaj et al., 2004) and functional dyspepsia (Tucker et al., 2012), as well as to determine residual volumes in preoperative sedation ahead of surgery (Lobo et al., 2009, Schmitz et al., 2012, Schmitz et al., 2011). However, practical issues such as non-standardised meals, time consuming image acquisition and manual analysis protocols have restricted the use of gastric MRI studies outside specialist research centres. A key barrier to implementation in clinical practice is the time required to analyze the data, for instance the measurement of gastric volumes from the scans by manual or assisted-manual (Barrett and Mortensen, 1996) drawing of the stomach content volume and air volume on every slice for every time point.

An additional complication is that gastric secretions within the stomach cannot be distinguished from the meal on standard MRI scans. Gastric secretion is highly variable between individuals and can complicate attempts to determine gastric meal volumes and, therefore, gastric emptying and nutrient delivery to the small bowel (Kwiatek et al., 2009). Gamma scintigraphy does not suffer from this problem as only the meal is labelled, but it cannot measure total gastric volume including intra-gastric air and secretions. This is important because total gastric volume has been closely linked to satiety scores of fullness in healthy individuals and patients with dyspepsia symptoms (Marciani et al., 2001b, Goetze et al., 2009, Treier et al., 2008, Parker et al., 2012c, Tucker et al., 2012). A variety of MRI techniques can be used to assess gastric secretion independent of meal volume. Early work measured changes in the MR relaxation time ( $T_2$ ) of locust bean gum solutions to estimate the amount of gastric secretions (Marciani et al., 2001b). More recently estimates of gastric secretion volume in liquid meals have been made by adding Gadolinium contrast agent to the meal which substantially reduces the  $T_1$  of the meal. This allows gastric secretion to be

measured from the change in  $T_1$  as the meal is diluted in the stomach (Goetze et al., 2009, Treier et al., 2008). However, published studies have used a dual flip angle sequence (and associated B1 map) to measure  $T_1$  which required an excessively long breath hold not tolerated by many patients.

This study presents a rapid MRI acquisition protocol and analysis algorithm suitable for the practical measurement of gastric volume and secretion volume in clinical studies. Throughout we aimed to minimise acquisition and analysis time without sacrificing measurement accuracy. Acquisition time was kept to a minimum with  $T_1$  maps generated from a respiratory triggered protocol that removed the need for prolonged breath holds during imaging. Semi-automatic volume analysis software was used to greatly reduce the time required to measure gastric volumes (Total Gastric Volume (TGV), gastric content volume (GCV) and intra-gastric air volume) and was applied to a study of the fate of a liquid meal swallowed by healthy volunteers. Reproducibility was assessed by the co-efficient of variance of the volumes measured by 3 observers. Measurement of gastric secretion and gastric meal volumes were validated by comparison of MRI measurements with gastric scintigraphy measurements that include only the labelled meal.

## Materials and Methods

An illustration and explanation of the terms used in this study and a flow diagram of the different meals and measurements taken are shown in figure 1.

### Meals

**Liquid Test Meal**—This meal was used in the assessment of total gastric volumes, gastric content volumes and intra-gastric air volumes. The meal was made up of 200ml vanilla fortisip (Nutricia Clinical) and 200ml water (300 kcal, 4.5 g fat /100ml). To this 0.4 mL of paramagnetic contrast agent was added (0.5 mmol/l Gd-DOTA; Dotarem®, Laboratoire Guerbet, Aulnay-sous-Bois, France) to increase the contrast between the meal and the surrounding tissues and to measure dilution (Parker et al., 2012b).

**Mixed Test Meal**—This meal was used in the assessment of secretion and meal only volumes. This contained the 400ml liquid test meal (above) with 12, 1% food grade agar beads (Marciani et al., 2001a) (Agar-agar; Cuisine-innovation: Dijon, France), which adds no nutrient value to the meal. 7.0g of barium sulphate per 100ml of agar solution (E-Z Paque: Buckinghamshire, UK, Ph Eur 96% w/w) was added to the agar beads to increase the density and prevent floating within the liquid meal (Parker et al., 2012a).

**Meal ingestion**—After baseline images had been acquired, at time  $T = -10$  mins, volunteers drank 200 ml of the liquid test meal at a rate of 100 ml/min and were then imaged ( $T = -5$  min). The remaining 200 ml of the test meal was consumed at a rate of 100 ml/min. If volunteers were consuming the mixed meal the agar beads were swallowed with the second 200 ml of liquid meal at a rate of 3 beads per 50 ml. Regular imaging commenced at  $T = 0$  mins

## Study Population

All healthy volunteers had no history of gastro-intestinal diseases and were suitable for MRI scanning. The volunteers gave written informed consent (LREC 10/H0408/52 liquid meal, 12/EM/0114 Mixed Meal) and arrived at the test centre after an overnight fast. All subjects abstained from alcohol and strenuous exercise for 24 h prior to each study day. 10 healthy volunteers (5 male, mean age 22, range 19-26 yrs) who had consumed the liquid test meal underwent the gastric volume measurement protocol (given below) and data were used to assess the fast analysis algorithm for measuring gastric volume (TGV, GCV and intra-gastric air). A further 24 healthy volunteers (male, mean age 48, range 19-69) who had consumed the mixed test meal underwent both the gastric volume and secretion protocols and data were used for assessing gastric secretion.

## MRI Study Protocol

Imaging was carried out using a Philips 1.5 T Achieva scanner with a 16 channel XL Torso Coil placed over the abdomen. Gastric volumes were determined from transverse balanced turbo field echo (bTFE) scans covering the stomach with 50 slices of 5mm thickness, no slice gap, in-plane resolution  $2.0 \times 1.77 \text{ mm}^2$ , FOV  $400 \times 320 \text{ mm}^2$ , TE/TR 1.5/3.0 ms, SENSE 2.0, FA  $80^\circ$ , data acquired in a short 16 s breath hold. Thin slices were used to reduce partial volume effects and a high flip angle was used to give good contrast between the fluid contents of the stomach and surrounding walls. Secretion volumes were estimated from  $T_1$  maps generated from a series of respiratory-triggered IR-EPI acquisitions (13 TIs 50-1000ms) (Cox et al., 2011) acquired with 5 slices of 8 mm thickness with slice gap of 5 mm, in plane resolution of  $3 \times 3 \text{ mm}^2$ , matrix size  $112 \times 112$ , SENSE factor 2.0, half scan factor 0.625, TE = 31 ms, TR minimum = 3000 ms. This method of  $T_1$  mapping allows data to be acquired relatively quickly without breath-holding. Triggering of the inversion pulse was altered with an additional variable delay to allow a range of TIs, whilst acquiring the images at the same time point within the late expiration phase of the respiratory cycle. Total acquisition time for this sequence ranged between 39-65 secs depending on the length of the respiratory cycle.

Scans to measure gastric volume were carried out before feeding, and at  $T = -5, 0, 5, 10, 15, 30, 45, 60, 75, 90, 120$  min after the whole meal had been consumed. Volume data at 60 min was only acquired after the mixed meal, and 3 subjects who consumed the liquid only meal did not have a scan at 45 min due to the constraints caused by interleaving of 2 subjects during acquisition.  $T_1$  maps to measure gastric secretion were acquired at 15 and 75 min after the meal.

To calibrate dilution against meal  $T_1$ , the  $T_1$  of the 400ml liquid test meal was measured during sequential dilution with simulated gastric secretions at  $37^\circ \text{C}$  (Rayment et al., 2009). This data was then fitted to the following equation to convert  $T_1$  into relative concentrations of meal and secretion.

$$\frac{1}{T_1} = \frac{1}{aC_{gd} + T_{1GS}} + (cC_{gd} + d) C_{gd} \quad \text{Eqn. 1}$$

where  $C_{gd}$  is the concentration of Gd-DOTA in  $\mu\text{M}$  and  $T_{IGS}$  the modelled  $T_1$  of pure gastric secretion (Treier et al., 2008), and  $a$ ,  $c$  and  $d$  are fitted parameters related to the baseline concentration of contrast agent, concentration dependence of the relaxivity of the contrast agent, and relaxivity of the undoped component of the meal.

## Image Analysis

**Gastric Volumes**—Software was written using IDL® 6.4 (Research Systems Inc, Boulder, Colorado, USA) to allow fast processing of the data to determine the content and intra-gastric air volume of the gastric lumen (Parker et al., 2012b). The algorithms used to define the contents and intra-gastric air (and hence total volume: intra-gastric air + contents) are described below.

**Gastric Contents Volume (GCV):** The observer started the analysis using data from a time point when the stomach was most full (e.g. between  $T = 0$  and 30 min). The observer defined a ‘seed’ point in the bright signal corresponding to the liquid phase of the meal and then moved a slider to define a minimum signal threshold. All voxels above this threshold connected to the seed point in the slice were used to define a binary mask. A closing filter (dilate then erode) of  $3 \times 3$  pixels was applied to this mask to fill any small holes within the region. The edge of the region was then displayed, allowing the observer to interactively refine the threshold to define the contents (see figure 2A-B). The final threshold level was saved and then seed points in the remaining slices including stomach contents were defined either manually (observer clicking) or automatically (new seed generated from centre of mass of previous slice’s mask, selected by the observer). After this had been repeated for all the slices showing stomach contents, three types of editing were applied as necessary.

1. Refining spatial limits. If the mask of the stomach had ‘leaked out’ where the stomach wall was very thin then the observer could draw a limit line which stopped the mask from extending in that direction (figure 2C-D).
2. Filling a hole. If there was a darker region within the stomach content which was not included within the mask (e.g. solid agar bead components or poorly mixed meal) then the observer could click within the hole and all the region inside the hole became part of the mask (Figure 2E-F).
3. Adding at the edge. If the threshold levels set did not include all the stomach contents at the edges, probably due to susceptibility artefacts, then the observer could draw on the correct edge and fill the corresponding hole created. (Figure 2G-H).

Additional editing was generally required only on a few slices per time point and this was not time-consuming since each hole was filled by a single ‘click’ and limits and edges were set with a ‘press-move-release’ action. After editing, the gastric contents were completely defined.

**Volume of Intra-gastric air:** The volume of intra-gastric air was defined using a similar method as for the contents except that a maximum signal threshold rather than a minimum signal threshold was used to define the dark area corresponding to air.

Finally, to ensure that pixels at the air/content boundary were handled properly, any voxel lying between the 2 masked regions in the vertical direction was assigned to the appropriate mask based on its signal intensity. Mean intensity levels of each region (intra-gastric air and contents separately) were calculated and the voxel was then assigned to the region having the closest intensity. The total number of voxels in each region in all slices were then calculated and converted to a volume using information on the voxel resolution.

*Total Gastric Volumes* (TGV) were computed from the sum of the gastric content and air volumes

For each volunteer the initial threshold levels were set according to the protocol above on the first data set analysed. These threshold levels (from the first data set analysed) were used for subsequent data sets of the same volunteer to increase the speed of analysis. However, occasionally, when the stomach was nearly empty, the signal intensity in the gastric contents became more heterogeneous and less bright, as the milk protein within the meal separated in the acidic environment and it was necessary to reduce the threshold intensity level for the accurate description of the contents to be completed.

**Gastric Secretions**—Maps of the  $T_1$  of the stomach content were generated on a voxel-by-voxel basis by a 3-parameter fit to the inversion recovery model

$$M_{TI} = M_0 \left( 1 - \alpha \exp \left( \frac{-TI}{T_1} \right) \right) \quad \text{Eqn 2}$$

using the Powell minimisation algorithm (Figure 3A-B), where  $M_{TI}$  is the signal at inversion time TI,  $M_0$  the equilibrium magnetisation and alpha is a parameter that takes account of the degree of inversion of the magnetization.  $R^2$  was also calculated for each voxel to determine the goodness of the fit. Images at long TI were used to determine the outline of the stomach, which was then defined manually by the observer, on all the slices and a histogram of  $T_1$  values within the region for voxels with an  $R^2$  of  $> 0.8$  was calculated with a bin size of 20 ms (figure 3C). Using a look up table of the data from the in-vitro calibration experiment each histogram bin was assigned to a percentage of meal and secretions (100 – meal %); e.g. 220 - 240 ms: 100% meal, 0 % secretions; 460 – 480 ms: 50% meal, 50 % secretion). The total volume of contents measured at that time point was then used to estimate the volume of meal ( $V_{meal}$ ) and volume of secretions ( $V_{sec}$ ) using the following equations

$$V_{meal} = \sum_{i=0}^n \frac{c_i \cdot V \cdot P_i}{100 \cdot N} \quad \text{Eqn. 3}$$

$$V_{sec} = \sum_{i=0}^n \frac{c_i \cdot V \cdot (100 - MP_i)}{100 \cdot N} \quad \text{Eqn. 4}$$

where  $c_i$  is the number of counts in histogram bin  $i$ ,  $V$  is the total volume measured at that time point from the bTFE images,  $n$  is the number of bins in the histogram,  $P_i$  is the percentage of meal corresponding to histogram bin  $i$  and  $N$  is the total number of counts in the histogram. For  $T = 15$  min  $n = 100$  corresponding to a maximum  $T_1$  of 2000 ms and for  $T=75$  min,  $n = 200$  corresponding to a maximum  $T_1$  of 4000 ms.



**Inter-observer Reproducibility**—To determine the variability of the volumes measured by different observers, 3 observers analysed all volume data from 10 healthy volunteers who had consumed the liquid test meal. Coefficient of variance for each volume measured was calculated and plotted against the mean volume measured by all three observers. This was done for TGV, GCV and intra-gastric air separately. Generation of the  $T_1$  map and subsequent estimated meal and secretion volumes were compared between 2 observers using Bland-Altman plots (Bland and Altman, 1999) for all data from the 24 healthy volunteers who had consumed the mixed meal.

**Accuracy of Secretion Estimations**—To determine whether the estimations of secretions were reasonable, the meal volumes were compared to Gamma Scintigraphy (GS) data obtained from the same subjects who ingested the same meal with a radionuclide tracer (on a separate occasion). The difference between gastric contents volume measured by MRI and GS provides an estimate of secretion volume because meal volumes calculated from MRI include secretion and those from GS do not. 0.5 MBq of the non-absorbable marker In-111-indium chloride was added to the liquid component of the meal and 5 MBq Tc-99m-MAA (Technescan® LyoMAA (DRN4378), Mallinckrodt Medical B.V., The Netherlands) to the agar beads. For imaging, radioactive markers were fixed to the subject at the right costal margin, both anteriorly and posteriorly. Subjects stood in front of a Mediso Gamma Camera (Nucline X-Ring-R, Budapest, Hungary) and a 30 s acquisition of anterior and posterior images were acquired.

The first 200 ml of the liquid test meal was given at 100ml/min and the subject was imaged (–5 min scan). The remaining liquid meal was then given at 100ml/min with 12 agar beads swallowed whole (3 beads per 50 ml). This two-stage technique allowed the In-111 overlap with the Tc-99 on the GS images to be corrected.

Meal volumes from GS at the same time points (T=15 and T=75 min) were compared to the MRI volumes (meal + secretions) as well as the meal only estimated volumes. Linear regression using data from both time points was used to compare the MR estimates of the meal volumes with and without secretions, to the volumes obtained from GS.

## Results

### Gastric Volumes

The semi-automatic algorithm for measuring stomach contents and air volumes required the observer to make far fewer mouse ‘clicks’ per image compared to manual, or assisted manual drawing. For a slice which required no editing, the air and contents could be defined by just 2 clicks compared to at least 7-10 per region for manual drawing. This reduced observer input, allowed faster processing, with typical times of 5-10 minutes to complete the volume analysis for the first volume (where threshold levels are set) for a stack of images covering the entire stomach; the timing depends on the amount of additional editing needed. For subsequent volumes where no threshold levels need to be set a typical dataset (contents and air) can be defined in 2-3 minutes. This results in a total processing time of 30-40 minutes for the full 12 time points.

The percentage coefficient of variance of volume measurements made by 3 observers can be seen in figure 4. The larger volumes had smaller coefficient of variance, since the differences between observers was generally at the very edges of the masks which has the smallest relative effect for large volumes. For content and total gastric volumes over 200 ml the mean (SD) percentage coefficient of variance was 3(2) % for TGV and 3(2) % for GCV. Volumes under 100 ml showed much larger percentage coefficient of variance as indicated on figure 4.

### Gastric Secretions

Data from the in-vitro dilution experiments are shown in figure 5. The fitted parameters of Eqn 1 for the dilution of the meal with simulated gastric secretions are as follows:

$$a = -1.4 \cdot 10^{-4} \text{ ms} \cdot \mu\text{M}^{-1}, T_{1GS} = 3830 \text{ ms}, c = 2.1 \cdot 10^{-8} \text{ ms}^{-1} \cdot \mu\text{M}^{-2}, d = 1.7 \cdot 10^{-5} \text{ ms}^{-1} \cdot \mu\text{M}^{-1}.$$

$T_1$  maps were successfully generated in all 24 subjects. Data were subsequently excluded in 5 data sets (N=3 at T=15 and N=2 at T=75 min) due to poor positioning of the slice stack in the antrum. A further 3 data sets from T=75 mins were also excluded due to poor fitting of the data. The mean (SD) number of voxels included in the histograms at T=15 mins was 2042 (640) and at T= 75 mins it was 1124 (461). The  $R^2$  constraint used to exclude voxels reduced the number of voxels by 18 (9) % for the T=15 min data and 25 (14) % for the T=75 min data, predominately from the edges of the regions, where wall motion generated errors in the data. The mean (SD) secretion volume at 15 min was 64 (51) ml and increased to 110 (40) ml by 75 min. Figure 6A shows that the total amount of secretion increased between the 2 time points for all subjects except one and the average amount of increase in secretion volume was 52 (29) ml. The two individuals with high levels of secretion at the earlier time point maintained this high level of secretion later.

### Accuracy of Secretion Estimations

The comparison of GCV and meal only volumes measured using MRI with gastric content volumes measured with GS is shown in figure 6B and mean values for the 2 time points are given in table 1. There was close agreement between MRI and GS meal volumes when the estimated volume of secretions was removed from the gastric contents volume data.

### Inter-Observer Variability

The inter-observer variability for gastric secretion measurements assessed using Bland-Altman plots, can be seen in figure 7. For the estimated secretion volumes there was a mean difference of -1 ml (CI -11 to 9 ml) between observers for T= 15 min and -1 ml (CI -16 to 14 ml) for the T= 75 min time points.

### Discussion

This paper reports the development and validation of a method for the rapid and reliable assessment of gastric meal and secretion volumes from magnetic resonance imaging (MRI). The findings demonstrate rapid secretion after consumption of this nutrient liquid test meal



that continues throughout the emptying process such that secretion contributes more than half the volume of the gastric contents 75 minutes after ingestion of this meal.

The algorithm proposed to measure gastric volumes significantly reduced the user input compared to manual drawing, even when manual drawing is assisted by a live-wire edge detection. Typical times for analysis for manually segmenting this data would be of the order of 3-4 hours, compared to 30-40 minutes using the semi-automated method. This allows data to be processed much faster. Reproducibility of results were maintained with minimal differences between results between three observers for gastric volumes exceeding 200ml, although the variation between observers increases as the gastric content volume reduces. This finding is due to the fact that the majority of inter-observer variation comes from setting the initial threshold level which primarily affects the edges of the region defined. This has a greater relative impact for smaller than larger gastric volumes, although the absolute volume differences were never large. Similar trends were previously reported by Fruehauf and colleagues (Fruehauf et al., 2011) where inter-observer variation for an alternative semi-automatic approach of gastric volumes was ~8% at 400ml, compared to ~3% found for the semi-automatic method described here. It should be noted that the relatively high percentage variation in measurements of gastric volumes at low volumes (< 100 mL) may not be critical in practice, because key metrics used to describe gastric function (e.g. half emptying time) are acquired early during gastric emptying. Moreover these measurements are derived from models that fit the entire emptying curve that can exclude or down weight later data points (Elashoff et al., 1982, Kwiatak et al., 2009). Further validation work will be needed to develop the software into a commercial package suitable for use in clinical practice.

This algorithm can also be applied to other liquid meals which show good contrast between the contents and stomach wall (Murray et al., 2013). It can also be used for meals containing solids such as the agar beads used in this study; however the thresholding method does not always work well if there is a large range of intensity levels across the stomach (e.g. after ingestion of a normal mixed meal) in which case further user input may be required to define the volumes accurately (Sweis et al., 2013). Recently there have been other semi-automatic algorithm proposed to segment intra-gastric contents and air by Banerjee et al (Banerjee et al., 2014) and Bharucha et al (Bharucha et al., 2014). The algorithm proposed by Bharucha follows a similar methodology to the one described in this work, as it uses both thresholding and morphological filtering with manual edits to achieve segmentation of the stomach and air and semi-automated analysis was completed in similar time scales (< 5 minutes per time point). However differences in the imaging sequences used to acquire data meant that residual gastric fluids present at baseline can also be assessed using the proposed segmentation algorithm as this fluid remained bright on the images, where it was dark for the Bharucha study. The Banerjee algorithm requires the observer to define a set of starting points throughout the volume of the stomach data which are at the boundaries of the contents and air. These starting points can be generated in several ways including thresholding (as used here). Once defined these points are used to define the edges of the regions automatically by using a live-wire boundary to connect adjacent points within each slice. This algorithm is also dependent on good contrast between the intra-gastric contents, air and the gastric walls. As a consequence it experiences similar problems to the algorithm

proposed here when contrast is poor. Further automation of the Banerjee algorithm allowing for consecutive time points to be processed assuming minimal changes to the shape and volume of the stomach and contents. The temporal resolution and possibility of large changes in position of the stomach within the imaging stack from repositioning of subjects may make the Banerjee algorithm less appropriate for clinical studies.

The original method used to quantify dilution via the  $T_1$  of gadolinium doped meals required prolonged breath-holds (Treier et al., 2008) which may not be practical for use with all patients, especially when combined with MRI volume scans which also require subjects to hold their breath. The rapid EPI sequence used in this study allows subjects to breath freely during the measurement of  $T_1$  potentially increasing the patient compliance and improving data quality in patients unable to hold their breath. An alternative method to measure both gastric volumes and gastric content  $T_1$  during free breathing has recently been proposed (Curcic et al., 2014b), using a golden angle radial sequence. In this study the meal and secretion volumes were highly reproducible between observers at both time points after the automatic removal of poorly fitted data at the very edges of the stomach where the quality of the  $T_1$  fit was reduced due to wall motion. The errors in measuring  $T_1$  from the observers are likely to be small when compared to other errors such as measurement reproducibility; however, these are hard to quantify as repeating measurements within the dynamics of gastric emptying is not appropriate. Treier et al (Treier et al., 2008) showed that the spread in  $T_1$  increased with increasing dilution of a test meal confined within an intra-gastric balloon and suggested that the accuracy of quantification of secretions would decrease with increasing  $T_1$ , although this would depend on the details of the  $T_1$  measurement protocol and to what extent it was optimal for measuring the short  $T_1$  of the meal. These technical issues may explain the unexpected drop in secretion level, seen between the  $T=15$  min and  $T=75$  min time points, in one of the subjects, who had a very high secretion volume, although as the total volume of this subject dropped over 200 ml in the 60 minutes between scans this drop in secretion may be a real effect due to rapid emptying of the secretion layer independent of the meal. A unique strength of the current study is that the accuracy of measurement of gastric meal and secretion volumes by MRI was validated by comparison to independent estimates of meal volume by gamma scintigraphy in the same subjects. Correcting the gastric content volume for the secretion volumes resulted in close agreement between measurements of meal volume by the two modalities, with a linear regression gradient close to 1 and intercept almost zero. The percentage difference in meal volume between the two measurement techniques was higher at 75 min because, as demonstrated by Fidler et al (Fidler et al., 2009), small changes in emptying rates between the two experimental days will have larger effects on the absolute volumes by the later time point.

The  $T_1$  mapping method does have some limitations. First, although EPI overcomes the problem of motion artefacts, the EPI readout, used in measuring secretions makes it difficult to obtain measurements in the antral area of the stomach due to artefacts from air distorting the images. As a result of this issue 5 out of the total 48 data sets had to be excluded due to poor positioning of the slice stack in this region. A further 3 data sets at the 75 min time point also had to be excluded due to poor fitting of the  $T_1$  data. Second, the poor spatial resolution of the EPI acquisition may result in errors in the  $T_1$  map at the edges of the stomach due to partial volume effects. Third this methodology is meal dependent, it works

best in meals that mix easily with the gastric secretions and would not necessarily be appropriate for other liquid meals that congeal, precipitate or phase separate in the acid environment. Fourth, small movements in the distal stomach wall also reduce the accuracy of volume measurements (a source of error for all imaging techniques)(Treier et al., 2008).

Another issue with the proposed methodology is that the area sampled does not cover the entire stomach, due to both wall movements and susceptibility artefacts in the distal stomach. This technique assumes that measurements acquired from the proximal stomach are applicable to the whole organ. However, in fact, at the early time point, there is layering of secretion in the stomach due to gravity which depends on body position. The proximal stomach will therefore contain relatively more meal and less secretion than the distal stomach and this is the probable reason for the small but significant systematic overestimation of meal volume / underestimation of secretion volume seen in Figure 6B at the 15 minute time point. It was also observed that the longest  $T_1$  and hence most concentrated gastric secretions were found at the stomach walls and formed a ring surrounding the liquid meal. By the 75 min time point the secretions are well mixed with the meal and the data from the proximal stomach should be a good representation of total gastric contents. All these observations confirmed previous results that have shown that the mixing of secretion into the meal takes time and is not homogeneous. Finally, it is worth noting that all MR relaxation time measurements are field strength dependent and measurements at 3.0 T would need separate in-vitro calibration data. The use of EPI acquisition at higher field strength would increase the image distortions, however alternative imaging sequences based on the bTFE acquisition could be used.

Notwithstanding these limitations, the proposed method has been shown to provide accurate measurements of gastric secretion that are sensitive to individual variation in secretion volumes, able to identify subjects that secreted large amounts of acid compared to those who secreted small amounts (Figure 6A). Moreover the histogram of the  $T_1$  maps provides visualisation of the mixing processes that occur during gastric emptying of a meal. More frequent scanning may be necessary if the kinetics of secretion and emptying are to be explored in more detail (Sauter et al., 2012). This technology may well have a role in clinical studies of reflux disease, functional dyspepsia and related disorders. (Curcic et al., 2014a, Tucker et al., 2012). Further it may be of great value in pharmacological studies that aim to either suppress gastric secretion or suppress gastro-esophageal reflux.(Sweis et al., 2013)

In conclusion we present an MRI acquisition and analysis protocol that provides accurate measurements of gastric volumes and secretion volumes with excellent inter-observer reproducibility for both variables. Gastric meal volumes obtained by this system were very similar to those obtained independently by gastric scintigraphy on a separate day. The protocol is patient friendly with rapid acquisition reducing the requirement to obtain data during breath-holding scans. Post-processing is rapid with a greatly reduced time required to derive measurements. Together these features provide the scientific basis of a protocol which would be suitable in clinical practice.

## References

- Ajaj W, et al. Real time high resolution magnetic resonance imaging for the assessment of gastric motility disorders. *Gut*. 2004; 53:1256–1261. [PubMed: 15306580]
- Banerjee S, et al. Validation of a rapid, semi-automatic Image analysis tool for measurement of gastric accommodation and emptying by magnetic resonance imaging. *Am J Physiol*. 2014 in press.
- Barrett WA, Mortensen EN. Fast, accurate, and reproducible live-wire boundary extraction. *Visualization in Biomedical Computing*. 1996; 1131:183–192.
- Bharucha AE, et al. Comparison of Manual and Semi-Automated Techniques for Analyzing Gastric Volumes with MRI in Humans. *Am J Physiol Gastrointest Liver Physiol*. 2014
- Bland JM, Altman DG. Measuring agreement in method comparison studies. *Statistical Methods in Medical Research*. 1999; 8:135–160. [PubMed: 10501650]
- Borovicka J, et al. Evaluation of gastric emptying and motility in diabetic gastroparesis with magnetic resonance imaging: effects of cisapride. *Am J Gastroenterol*. 1999; 94:2866–73. [PubMed: 10520835]
- Cox, EF.; Hoad, CL.; Francis, SF. Quantification of renal T1 using a modified respiratory triggered inversion recovery TrueFISP scheme [Abstract]; 19th Annual Meeting of the ISMRM; Montreal. 2011; 825
- Curcic J, et al. Gastroesophageal junction: structure and function as assessed by using MR imaging. *Radiology*. 2010; 257:115–24. [PubMed: 20713610]
- Curcic J, et al. Abnormal structure and function of the esophagogastric junction and proximal stomach in gastroesophageal reflux disease. *Am J Gastroenterol*. 2014a; 109:658–67. [PubMed: 24589669]
- Curcic J, et al. Validation of a golden angle radial sequence (GOLD) for abdominal T1 mapping during free breathing: Demonstrating clinical feasibility for quantifying gastric secretion and emptying. *J Magn Reson Imaging*. 2014b doi 10.1002/jmri.24530. [PubMed: 24391022]
- Elashoff JD, Reedy TJ, Meyer JH. Analysis of Gastric-Emptying Data. *Gastroenterology*. 1982; 83:1306–1312. [PubMed: 7129034]
- Fidler J, et al. Application of magnetic resonance imaging to measure fasting and postprandial volumes in humans. *Neurogastroenterol Motil*. 2009; 21:42–51. [PubMed: 19019018]
- Fruehauf H, et al. Inter-observer reproducibility and analysis of gastric volume measurements and gastric emptying assessed with magnetic resonance imaging. *Neurogastroenterol Motil*. 2011; 23:854–61. [PubMed: 21740482]
- Fruehauf H, et al. Characterization of gastric volume responses and liquid emptying in functional dyspepsia and health by MRI or barostat and simultaneous C-acetate breath test. *Neurogastroenterol Motil*. 2009; 21:697–e37. [PubMed: 19368659]
- Goetze O, et al. The effect of gastric secretion on gastric physiology and emptying in the fasted and fed state assessed by magnetic resonance imaging. *Neurogastroenterol Motil*. 2009; 21:725–e42. [PubMed: 19344341]
- Kwiatek MA, et al. Effect of meal volume and calorie load on postprandial gastric function and emptying: studies under physiological conditions by combined fiber-optic pressure measurement and MRI. *Am J Physiol Gastrointest Liver Physiol*. 2009; 297:G894–901. [PubMed: 19779010]
- Kwiatek MA, et al. Quantification of distal antral contractile motility in healthy human stomach with magnetic resonance imaging. *J Magn Reson Imaging*. 2006; 24:1101–9. [PubMed: 17031837]
- Lobo DN, et al. Gastric emptying of three liquid oral preoperative metabolic preconditioning regimens measured by magnetic resonance imaging in healthy adult volunteers: a randomised double-blind, crossover study. *Clin Nutr*. 2009; 28:636–41. [PubMed: 19500889]
- Marciani L. Assessment of gastrointestinal motor functions by MRI: a comprehensive review. *Neurogastroenterol Motil*. 2011; 23:399–407. [PubMed: 21276139]
- Marciani L, et al. Gallbladder contraction, gastric emptying and antral motility: single visit assessment of upper GI function in untreated celiac disease using echo-planar MRI. *J Magn Reson Imaging*. 2005; 22:634–8. [PubMed: 16193473]

- Marciani L, et al. Assessment of antral grinding of a model solid meal with echo- planar imaging. *American Journal of Physiology-Gastrointestinal and Liver Physiology*. 2001a; 280:G844–G849. [PubMed: 11292591]
- Marciani L, et al. Effect of meal viscosity and nutrients on satiety, intragastric dilution, and emptying assessed by MRI. *American Journal of Physiology-Gastrointestinal and Liver Physiology*. 2001b; 280:G1227–G1233. [PubMed: 11352816]
- Marciani L, et al. Preventing gastric sieving by blending a solid/water meal enhances satiation in healthy humans. *J Nutr*. 2012; 142:1253–8. [PubMed: 22649258]
- Marciani L, et al. Delayed gastric emptying and reduced postprandial small bowel water content of equicaloric whole meal bread versus rice meals in healthy subjects: novel MRI insights. *Eur J Clin Nutr*. 2013; 67:754–8. [PubMed: 23594839]
- Marciani L, et al. Magnetic resonance imaging (MRI) assessment of gastric emptying and antral motility in clinical practice: Preliminary results on patients. *Gastroenterology*. 2000; 118:2056.
- Marciani L, et al. Enhancement of intragastric acid stability of a fat emulsion meal delays gastric emptying, increases cholecystokinin release and gallbladder contraction. *Am J Physiol Gastrointest Liver Physiol*. 2007; 292:G1607–13. [PubMed: 17332474]
- Marciani L, et al. Antral motility measurements by magnetic resonance imaging. *Neurogastroenterology and Motility*. 2001c; 13:511–518. [PubMed: 11696113]
- Murray K, et al. Differential Effects of FODMAPs (Fermentable Oligo-, Di-, Mono-Saccharides and Polyols) on Small and Large Intestinal Contents in Healthy Subjects Shown by MRI. *Am J Gastroenterol*. 2013; 109:110–119. [PubMed: 24247211]
- Parker H, et al. Development and validation of a mixed liquid/solid test meal for use in clinical practice. *Neurogastroenterology and Motility*. 2012a; 24:167.
- Parker HL, et al. Validation of a Novel, Non-Invasive Assessment of Gastric Function and Gastric Emptying (GE) After a Large Liquid Nutrient Meal by Magnetic Resonance Imaging (MRI). *Gastroenterology*. 2012b; 142:S610–S610.
- Parker HL, et al. Effects of Age, Sex and Obesity on Satiation Assessed by Nutrient Drink Test and Gastric Emptying (GE) Assessed by Non-Invasive Gastric Scintigraphy (GS) and Magnetic Resonance Imaging (MRI): Analysis and Comparison of Methods. *Gastroenterology*. 2012c; 142:S293–S293.
- Rayment P, et al. Investigation of alginate beads for gastro-intestinal functionality, Part 1: In vitro characterisation. *Food Hydrocolloids*. 2009; 23:816–822.
- Sauter M, et al. Measuring the interaction of meal and gastric secretion: a combined quantitative magnetic resonance imaging and pharmacokinetic modeling approach. *Neurogastroenterol Motil*. 2012; 24:632–8. e272–3. [PubMed: 22452723]
- Schmitz A, et al. Residual gastric contents volume does not differ following 4 or 6 h fasting after a light breakfast - a magnetic resonance imaging investigation in healthy non-anaesthetised school-age children. *Acta Anaesthesiol Scand*. 2012; 56:589–94. [PubMed: 22188334]
- Schmitz A, et al. Fasting times and gastric contents volume in children undergoing deep propofol sedation--an assessment using magnetic resonance imaging. *Paediatr Anaesth*. 2011; 21:685–90. [PubMed: 21414079]
- Schwizer W, Maecke H, Fried M. Measurement of gastric emptying by magnetic resonance imaging in humans. *Gastroenterology*. 1992; 103:369–76. [PubMed: 1634055]
- Steingøtter A, et al. Effects of posture on the physiology of gastric emptying: a magnetic resonance imaging study. *Scand J Gastroenterol*. 2006; 41:1155–64. [PubMed: 16990200]
- Sweis R, et al. Post-prandial reflux suppression by a raft-forming alginate (Gaviscon Advance) compared to a simple antacid documented by magnetic resonance imaging and pH-impedance monitoring: mechanistic assessment in healthy volunteers and randomised, controlled, double-blind study in reflux patients. *Aliment Pharmacol Ther*. 2013; 37:1093–102. [PubMed: 23600790]
- Treier R, et al. Fast and optimized T1 mapping technique for the noninvasive quantification of gastric secretion. *J Magn Reson Imaging*. 2008; 28:96–102. [PubMed: 18581398]
- Tucker E, et al. Gastric Volume Responses and Emptying After a Large Liquid Nutrient Meal in Functional Dyspepsia and Health Assessed by Non-Invasive Gastric Scintigraphy (GS) and

Magnetic Resonance Imaging (MRI): A Pilot Study to Identify Candidate Biomarkers.  
Gastroenterology. 2012; 142:S194–S194.

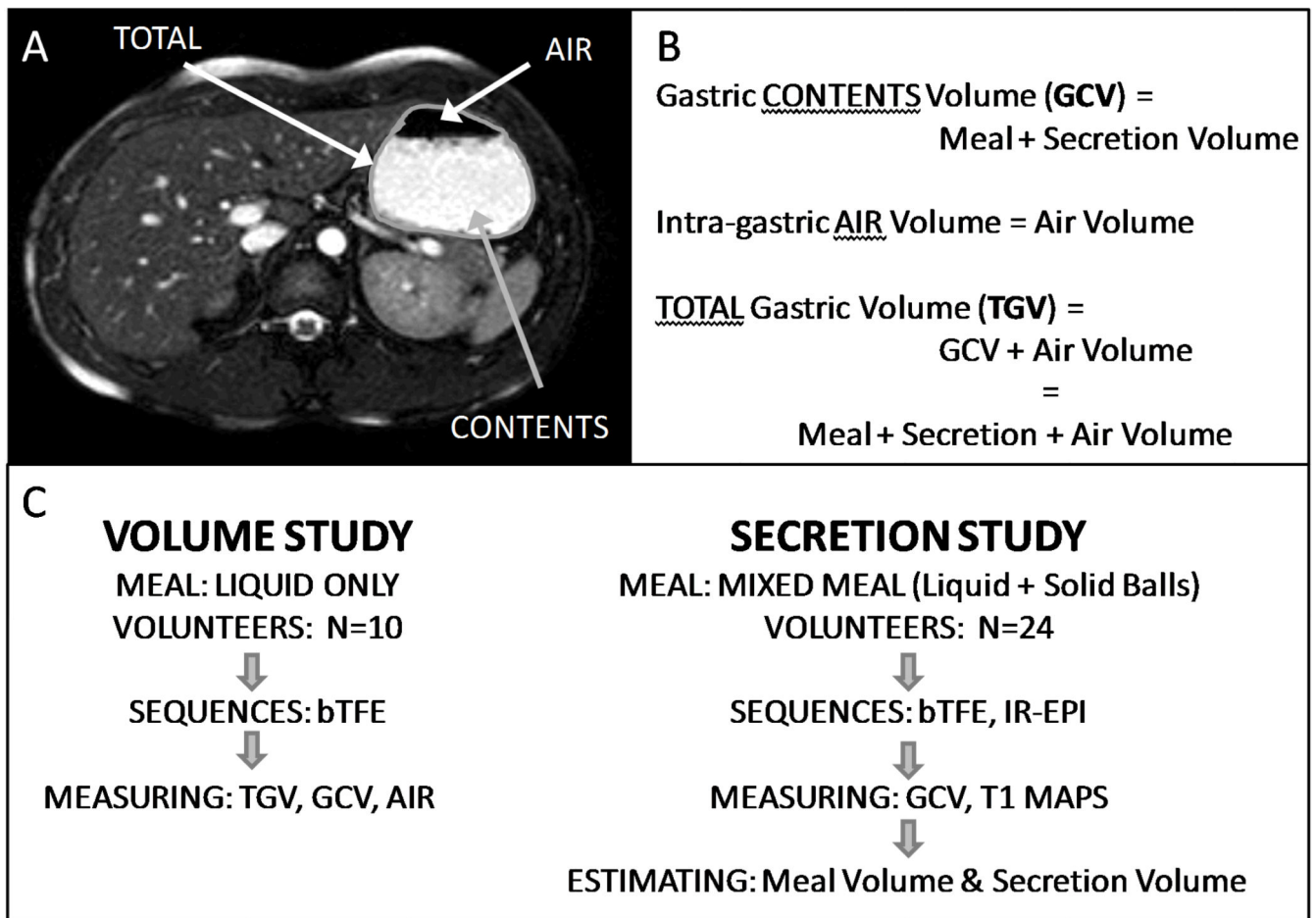


**Figure 1.**

A representative image of the stomach is presented (A) with an explanation of the terms used in this study (B) and a flow diagram of the different meals and measurements taken in the volume and secretion studies (C).



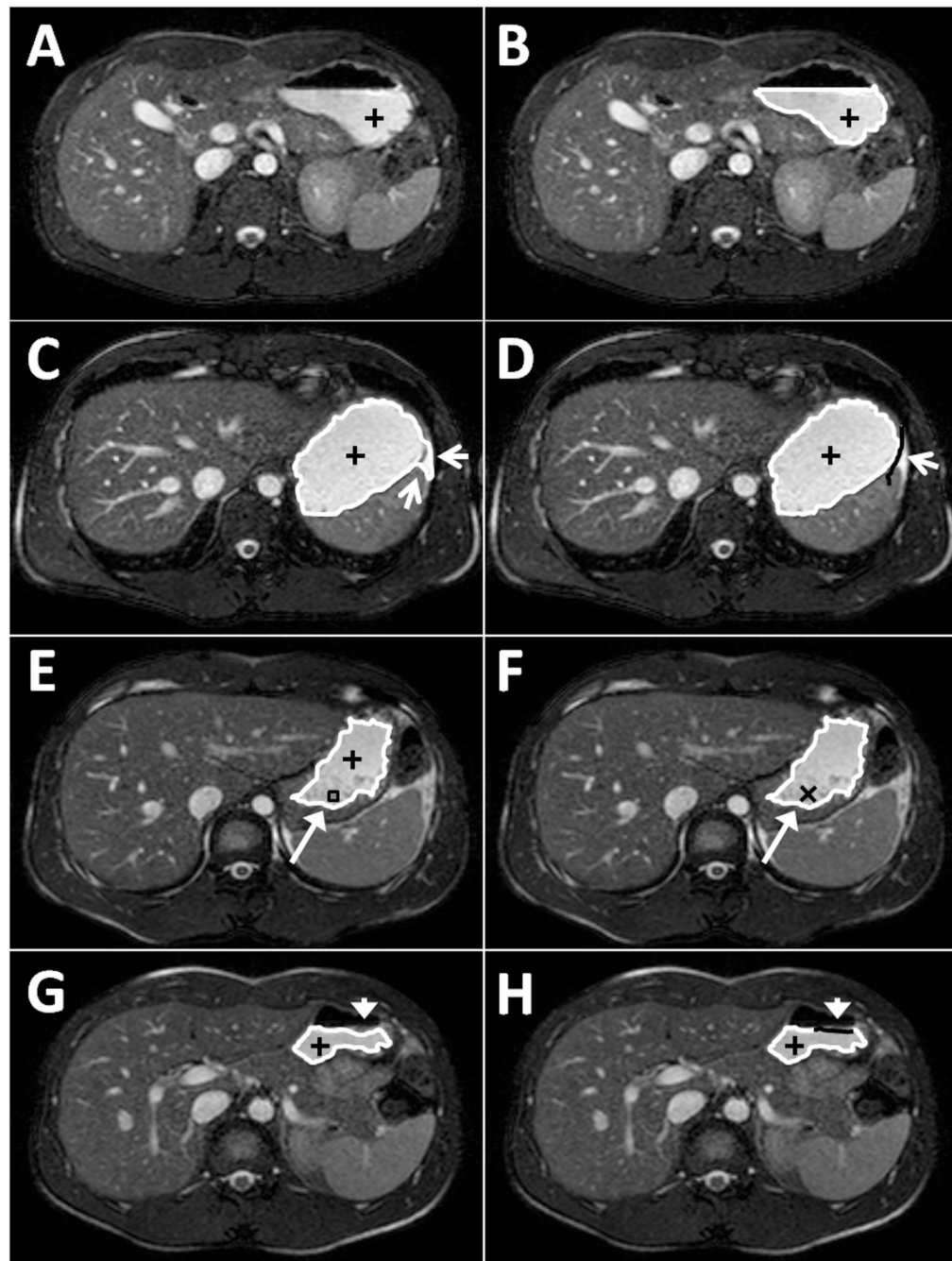


**Figure 2.**

Illustrations of the post-processing analysis algorithm for measurement of gastric volumes. (A) First seed point is positioned in the stomach (black plus sign). (B) Minimum threshold level correctly set so that edges (white line) of the mask defined are at the edges of the stomach contents. (C) Example of mask 'leaking out' of stomach (white arrows). (D) Example of observer defined correction for 'leaking out' by setting a limit on the slice (solid black line). (E) Example of a hole in the mask (long white arrow, black box). (F) Hole has been filled by clicking inside it (black cross). (G) Example of edge missing from mask

defined (white arrow head). (H) Observer has corrected edge (solid black line) by adding the edge in the correct place.

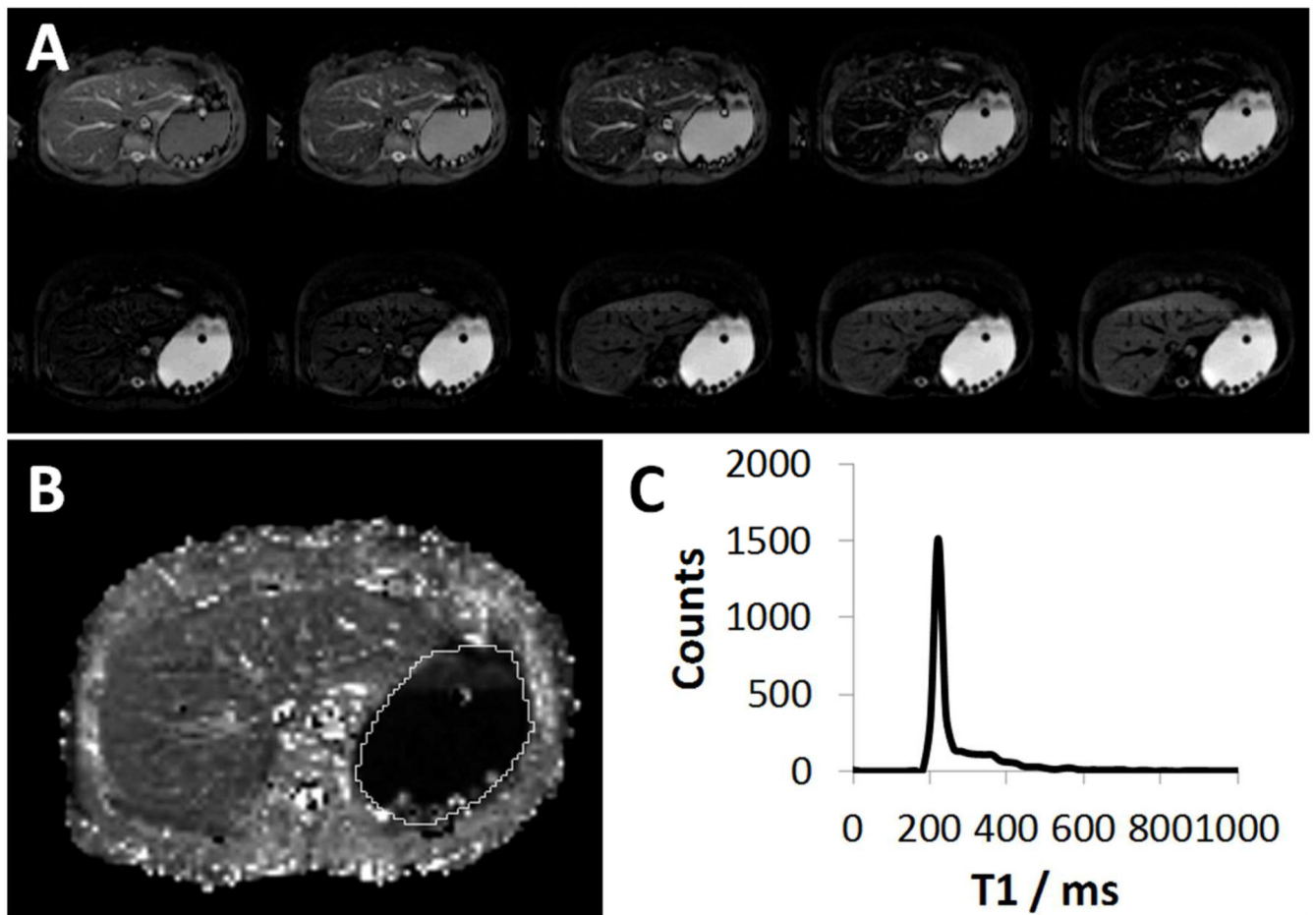


**Figure 3.**

(A) Example of raw IR-EPI images at increasing TI times for a single slice through the main body of the stomach. (B)  $T_1$  map of the corresponding slice shown in (A), with stomach region defined (white line). (C) Histogram of stomach region showing distribution of  $T_1$  data from all slices acquired. Note the inhomogeneous distribution of secretions in the stomach. There is a layer of secretion (i.e. highly dilute gastric contents) that is clearly visible above the Gd-labelled meal on (B) with the undiluted meal reflected by a narrow peak in the distribution of  $T_1$  data in the histogram (C) and the dilute region reflected by the visible plateau beyond the peak.

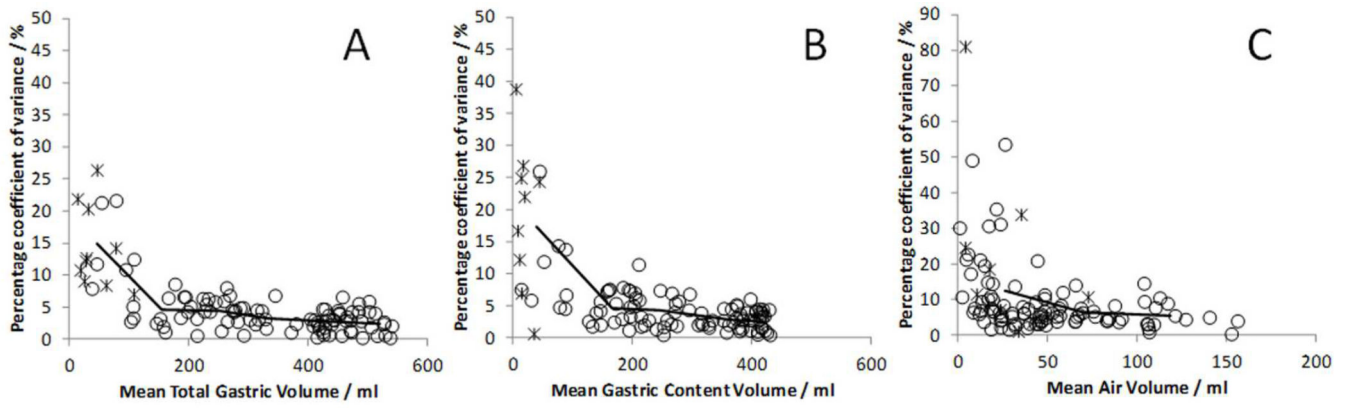


**Figure 4.**

Graphs showing the percentage coefficient of variance against mean volumes for (A) Total Gastric Volume, (B) Gastric Content Volume (C) Air Volume. Lines drawn through data show means of data split by volume; TGV and GCV averaged per 100 ml of volume, Air averaged per 50 ml of volume. Data during meal ingestion and post-ingestion shown as circles and crosses.

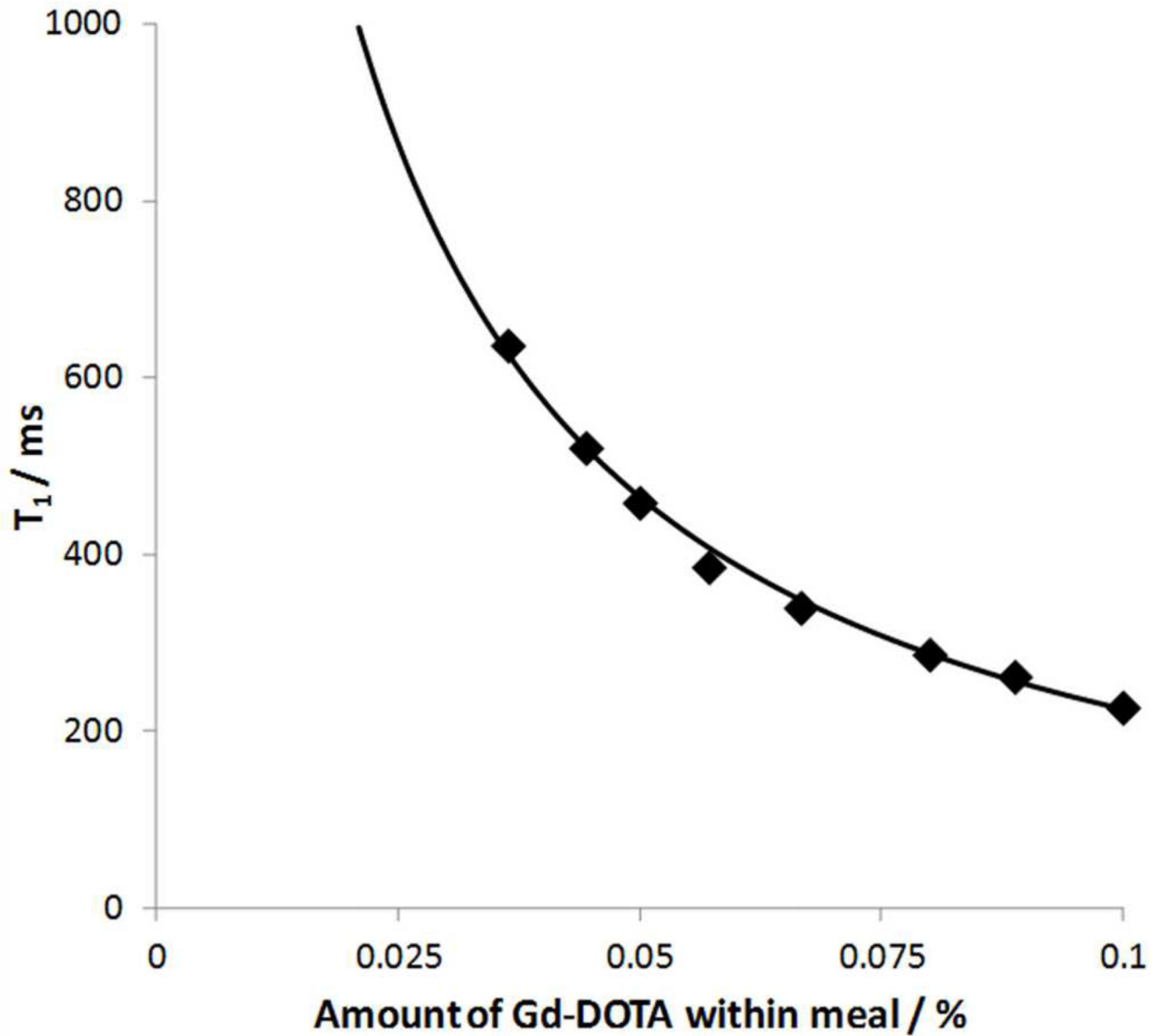


**Figure 5.**

Graph showing  $T_1$  measured from dilution of liquid test meal with simulated gastric secretions. Data, fitted to Eqn 1 is shown as solid line.

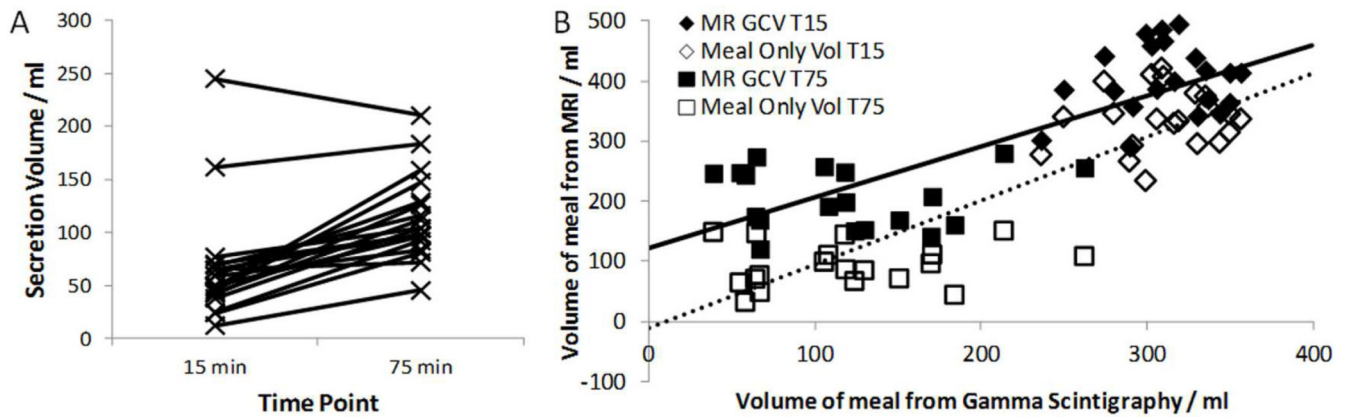


**Figure 6.**

(A) Individual estimates of secretion volumes for both time points measured from the dilution scan. (B) Graph comparing MRI estimates of GCV and meal only volume to gamma scintigraphy estimates of the remaining meal volume. Linear regression of MRI volumes with GS volumes also shown, solid line: GCV, dotted line: meal only volumes. Note that the MRI meal volume measurements corrected for secretion lies close to the line of identity suggesting that the values closely agree with the meal volume calculated from GS counts.

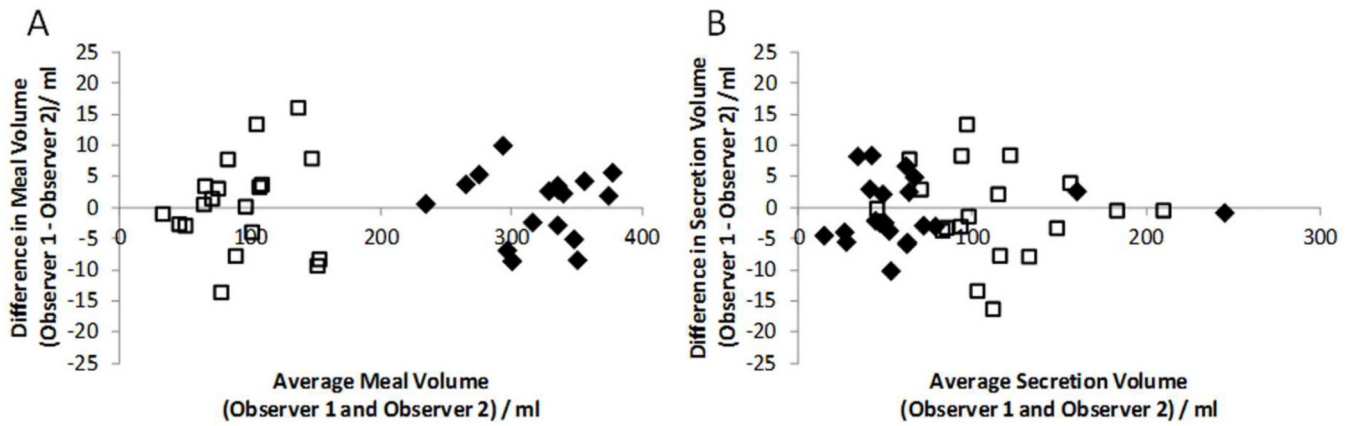


**Figure 7.**

Graphs showing Bland Altman plots of estimated meal volumes (A) and secretions (B) for 2 observers. T15 shown as solid diamonds, T75 shown as open squares. Differences in gastric contents volume measured following ingestion of a 400ml meal were usually less than 10ml.



**Table 1**

Comparison of volume data from MRI and GS and linear regression of gastric MRI against Gastric Scintigraphy (GS).

	Mean Volume (SD) / ml		Linear Regression and Correlation with GS data		
	T = 15 mins	T = 75 mins	Gradient (std err)	Intercept (std err)	Pearson Correlation Coefficient
GCV MRI	402 (58)	202 (50)	0.85 (0.10)	121 (25)	0.808 <sup>‡</sup>
Meal only volume MRI*	338 (50)	92 (36)	1.06 (0.10)	-11 (24)	0.867 <sup>‡</sup>
Meal volume GS	310 (32)	112 (61)			

\* This data has been corrected removing the estimated secretion volume from the GCV.

<sup>‡</sup> Significant to  $p < 0.001$  N=40.